

# Rheological and Structural Properties of Aqueous Alginate during Gelation via the Ugi Multicomponent Condensation Reaction

Huaitian Bu,<sup>†</sup> Anna-Lena Kjøniksen,<sup>†</sup> Kenneth D. Knudsen,<sup>‡</sup> and Bo Nyström<sup>\*,†</sup>

Department of Chemistry, University of Oslo, P.O. Box 1033, N-0315 Oslo, Norway, and Department of Physics, Institute for Energy Technology, N-2027 Kjeller, Norway

Received January 22, 2004; Revised Manuscript Received April 1, 2004

Turbidity, structure, and rheological features during gelation via the Ugi multicomponent condensation reaction of semidilute solutions of alginate have been investigated at different polymer and cross-linker concentrations and reaction temperatures. The gelation time of the system decreased with increasing polymer and cross-linker concentrations, and a temperature rise resulted in a faster gelation. At the gel point, a power law frequency dependence of the dynamic storage modulus ( $G' \propto \omega^n$ ) and loss modulus ( $G'' \propto \omega^n$ ) was observed for all gelling systems with  $n' = n'' = n$ . By varying the cross-linker density at a fixed polymer concentration (2.2 wt %), the power law exponent is consistent with that predicted (0.7) from the percolation model. The value of  $n$  decreases with increasing polymer concentration, whereas higher temperatures give rise to higher values of  $n$ . The elastic properties of the gels continue to grow over a long time in the postgel region, and at later stages in the gelation process, a solidlike response is observed. The turbidity of the gelling system increases as the gel evolves, and this effect is more pronounced at higher cross-linker concentration. The small-angle neutron scattering results reveal large-scale inhomogeneities of the gels, and this effect is enhanced as the cross-linker density increases. The structural, turbidity, and rheological features were found to change over an extended time after the formation of the incipient gel. It was demonstrated that temperature, polymer, and cross-linker concentrations could be utilized to tune the physical properties of the Ugi gels such as structure, transparency, and viscoelasticity.

## Introduction

Polymeric hydrogels belong to a class of materials that can swell largely in water and maintain their three-dimensional network structure in the swollen state. The mechanical, solvent permeability, swelling, and hydrophilic/hydrophobic properties of a hydrogel can be modulated by choice of type of polymer/monomer and method of synthesis. Among biopolymers that can form hydrogels are alginate, collagen, and chitosan. These polymers are biocompatible and attractive in the development of potential materials for drug release systems and tissue engineering.<sup>1,2</sup>

Alginate is regarded as a nontoxic, nonimmunogenic, and biodegradable polymer, which makes it an attractive candidate for biomedical applications. This macromolecule is an anionic copolymer, comprised of  $\beta$ -D-mannuronic acid (M-block) and (1 $\rightarrow$ 4)-linked  $\alpha$ -L-guluronic acid (G-block) units arranged in a nonregular blockwise pattern of varying proportion of GG, MG, and MM blocks.<sup>3</sup> The chemical structure of alginate is shown in Figure 1. The physical properties of alginates depend not only upon the uronic acid composition but also on the relative proportion of the three-block types.<sup>4</sup>

Alginate is known to form a hydrogel in the presence of divalent cations, such as calcium ( $\text{Ca}^{2+}$ ), which act as cross-

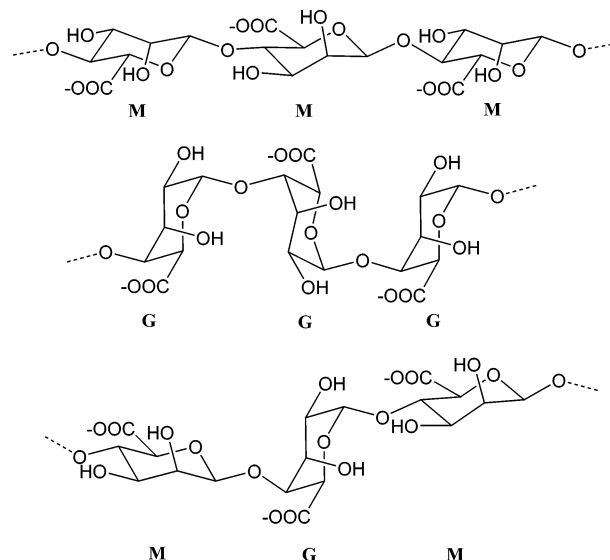


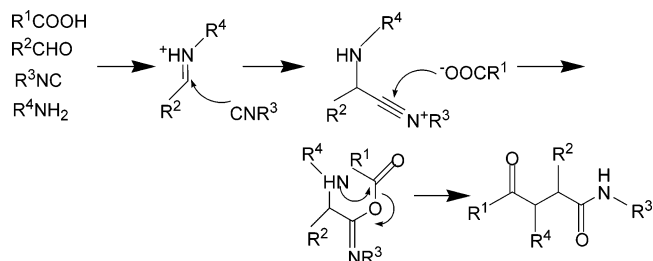
**Figure 1.** Chemical structure units of alginate (M = mannuronic acid and G = guluronic acid).

linkers between the functional groups of alginate chains. Besides hydrogels induced by divalent cations, alginate can form acid gels at pH below the  $\text{pK}_a$  value of the uronic acid residues.<sup>5</sup> By adding the slowly hydrolyzing D-glucono- $\delta$ -lactone (GDL), alginate is acidified and forms alginic acid gel.<sup>6</sup> These gels have been proposed to be stabilized by intermolecular hydrogen bonds.<sup>7</sup>

\* To whom correspondence should be addressed.

<sup>†</sup> University of Oslo.

<sup>‡</sup> Institute for Energy Technology.

**Scheme 1.** Ugi Condensation Reaction Mechanism

An alternative strategy to form hydrogels is through chemical cross-linking reactions. Alginate contains carboxylic acid and hydroxyl groups, and both of them can be used as functionalities to form covalent cross-links. Ester linkages can be formed between carboxylic acid and hydroxyl groups of alginate by using water-soluble carbodiimide as the cross-linking agent.<sup>8</sup> However, the ester bond is prone to hydrolysis, and it is therefore not stable.<sup>9,10</sup> Mooney et al.<sup>11,12</sup> have reported cross-linking alginate with poly(ethylene glycol)-diamines. By controlling either the chain length of the cross-linking molecule or the cross-linking density, hydrogels with different mechanical properties have been produced. Cross-linkers with different sizes and structures, including adipic dihydrazide and lysine, have also been utilized in the development of alginate hydrogels.<sup>12</sup> The results show that the mechanical properties of the hydrogels are mainly controlled by the cross-linking density, but they are also moderately dependent on the type of cross-linking molecules. The general picture that emerges for cross-linked alginate gels is that it is possible to control the rheological features of the systems by changing the type of cross-linking agent and the length of the cross-linked junctions.<sup>13</sup> Gelation of semidilute alginate solutions could be accomplished via ionic or covalent cross-linking. It was found that increased density of covalent cross-links yielded higher values of the elastic modulus and more brittle gels were formed. Using ionic or covalent cross-linking and varying the cross-linking density can tune the mechanical features of hydrogels.

Although the gel-forming methods mentioned above produce alginate hydrogels with versatile properties, they all involve labor-consuming work in the modification of alginate or the synthesis of a cross-linker. A more simple and direct procedure for the synthesis of chemical hydrogels is the Ugi multicomponent condensation reaction on carboxylated polysaccharides.

In the Ugi four-component condensation reaction,<sup>14</sup> the reaction mixture contains an amine, which condenses with the carbonyl group to yield an imine (see Scheme 1). The protonated imine and the carboxylate react with the isocyanide to give an  $\alpha$ -(acylamino) amide. This procedure has been used for the synthesis of an alginate-based network for the immobilization of an enzyme.<sup>15</sup> It has been shown that, by using a bifunctional cross-linker, hydrogels with diamide linkages between the chains can be formed. For instance, Crescenzi et al.<sup>16</sup> have used lysine ethyl ester as a cross-linker diamine in a reaction with hyaluronic acid to prepare a hydrogel. De Nooy et al.<sup>17,18</sup> have utilized the Ugi and Passerini reactions to form hydrogels from polysaccharide solutions. In the Ugi reaction, amide linkages are formed

between the polysaccharide chains, whereas the Passerini reaction yields ester linkages. Since the ester linkage can be easily hydrolyzed at only slightly alkaline pH, whereas the amide linkage is stable at alkaline conditions, this difference is an important distinction between the two types of reactions.

In this work, alginate hydrogels are prepared via the Ugi reaction, using 1,5-diaminopentane (DAP) as the bifunctional cross-linker agent. The effects of alginate concentration, cross-linking density, and reaction temperature during the gelation reactions of alginate solutions have been investigated with the aid of oscillatory shear, turbidity, and small angle neutron scattering (SANS) experiments. We will show how the temperature, cross-linker, and polymer concentrations affect the rheological characteristics of the system as the Ugi gels of alginate evolve. Aspects of the transparency and structure of the gels will also be given. The aim of this study is to gain insight into changes of the rheological, thermodynamic, and structural features of the system during the gelation process at various conditions. We believe that these results will provide us with a more detailed picture of the characteristic features of Ugi gels. To the best of our knowledge, this is the first systematic investigation of fundamental physical properties of gelling alginate systems, prepared via the Ugi condensation reaction.

## Experimental Section

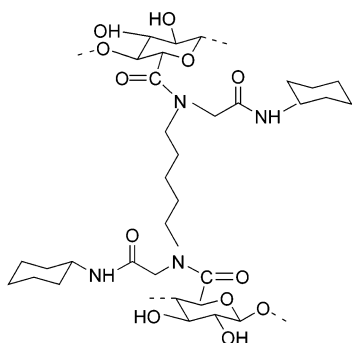
**Materials.** An alginate sample, designated LF 10/60 LS (# 912912), was supplied by FMC Biopolymers, Drammen, Norway. According to the specifications from the manufacturer, this sample has a weight-average molecular weight of 152 000 and the guluronic acid to mannuronic acid (G/M) ratio is 0.75. The  $pK_a$  values of G and M have been determined to 3.7 and 3.4, respectively.<sup>19</sup>

Alginate solutions were dialyzed against pure water for several days to remove salt and other low-molecular weight impurities and were thereafter freeze-dried. Regenerated cellulose with a molecular weight cutoff of 8000 was used as the dialyzing membrane. By this procedure, the brownish-yellow color of the solutions disappeared.

Hydrochloric acid, formaldehyde, 1,5-diaminopentane (DAP), and cyclohexyl isocyanide were purchased from Merck or Fluka and were of analytical grade. These chemicals were used without any further purification. Double distilled Millipore water was utilized in this work.

**Preparation of Solutions and Gel Formation.** The polymer was dissolved in water at room temperature by weighing the components, and it was gently stirred overnight to obtain homogeneous solutions. The resulting solution was slightly acidified with dilute HCl solution to obtain the acidity (a pH of approximately 3.6) necessary for the Ugi reaction to proceed,<sup>18</sup> and water was added to obtain the desired polymer concentration. The polymer concentrations are expressed in terms of weight percentage of polymer.

Formaldehyde, 1,5-diaminopentane, and cyclohexyl isocyanide were added to the solution successively. After the addition of each component, the solution was stirred vigorously to disperse the component homogeneously in the solution. The molar amount of bifunctional cross-linker DAP

**Scheme 2.** Possible Cross-Link Formed by an Ugi Reaction for Alginate

was calculated with respect to the molar amount of carbohydrate monomers; thus determining the theoretical cross-linking density. The other components were added in an excess of about 40%. A possible linkage formed with alginate is represented in Scheme 2. After the last component cyclohexyl isocyanide was added, the solution was stirred and then loaded in the rheometer for the oscillatory shear measurements, or other types of experiments were carried out. Except for the rheological measurements of the effects of reaction temperature on the gelation process, all of the other experiments were conducted at 25 °C.

**pH Measurements.** The pH values of the acidified alginate solutions and the gelling systems were determined by using a PHM210 standard pH meter (Radiometer Analytical S. A., France) at the considered temperatures. The pH of the adjusted alginate solutions was about 3.6, whereas the final pH of the systems, after addition of the basic DAP component, was typically 8.5.

**Rheological Experiments.** Oscillatory sweep measurements were carried out in a Paar-Physica MCR 300 rheometer using a cone-and-plate geometry, with a cone angle of 1° and a diameter of 75 mm. The samples were applied on the plate, and a thin layer of low-viscosity silicone oil was used to cover the free surface of the solution to prevent evaporation of solvent. The values of strain amplitude were checked to ensure that all measurements were conducted in the linear viscoelastic regime, where the dynamic storage modulus ( $G'$ ) and loss modulus ( $G''$ ) are independent of the strain amplitude. The measurements were performed over an extended angular frequency ( $\omega$ ) domain. The measuring device is equipped with a temperature unit (Peltier plate) that provides a rapid change of the temperature and gives a very good temperature control over an extended time.

**Analysis of Rheological Data.** A simple power law can describe the rheological behavior of an incipient gel, where the dynamic moduli are related as<sup>20</sup>

$$G' = G''/\tan \delta = S\omega^n \Gamma(1 - n) \cos \delta \quad (1)$$

where  $\Gamma(1 - n)$  is the gamma function,  $n$  is the relaxation exponent, and  $S$  is the gel strength parameter, which depends on the cross-linking density and the molecular chain flexibility.<sup>20</sup> This relationship has been utilized in this work to calculate the values of the  $S$  parameter. However, values of  $S$  can also be calculated from the absolute value of complex viscosity (see eq 5) and this method yields consistent results.

The phase angle ( $\delta$ ) between stress and strain is independent of frequency ( $\omega$ ) but proportional to the relaxation exponent

$$\tan \delta = G''/G' = \tan(n\pi/2) \quad (2)$$

These results suggest that the following scaling relation can describe the incipient gel:

$$G'(\omega) \propto G''(\omega) \propto \omega^n \quad (3)$$

However, if the dynamic moduli exhibit a very weak frequency dependence, it is convenient to follow the evolution of the rheological properties during gelation through the complex viscosity, with its absolute value  $|\eta^*(\omega)|$  given by

$$|\eta^*(\omega)| = (G'^2 + G''^2)^{1/2}/\omega \quad (4)$$

In an analogous way as for the dynamic moduli, we may describe the frequency dependence of the absolute value of complex viscosity at the gel point ( $t_g$ ) in terms of a power law<sup>21</sup>

$$|\eta^*(\omega)| = aS\omega^m \quad (5)$$

with

$$m = n - 1 \quad (6)$$

and

$$a = \frac{\pi}{\Gamma(n) \sin(n\pi)} \quad (7)$$

where  $m$  is related to the exponent  $n$ . It is clear that, if the frequency dependence of the dynamic moduli is weak ( $n$  is close to 0), a strong, easily detected dependency of  $m$  ( $m$  approaches  $-1$ ) is expected. Values of  $m$  close to zero indicate liquidlike behavior, whereas values of  $m$  approaching  $-1$  suggest solidlike response.

**Turbidity Measurements.** Turbidities of alginate solutions during the gelation process were measured with a Helios Gamma (Thermo Spectronic, Cambridge, U.K.) spectrophotometer at a wavelength of 500 nm, and the transmittance was recorded. The apparatus is equipped with a temperature unit (Peltier plate) that gives a very good temperature control over an extended time. The turbidity  $\tau$  of the samples can be determined from the following relationship:

$$\tau = (-1/L) \ln(I_t/I_0) \quad (8)$$

where  $L$  is the light path length in the cell (1.0 cm),  $I_t$  is the transmitted light intensity, and  $I_0$  is the incident light intensity.

**Small-Angle Neutron Scattering (SANS).** Small-angle neutron scattering experiments were carried out at 25 °C at the SANS installation at the IFE reactor at Kjeller, Norway. The instrument is equipped with a liquid hydrogen moderator, which shifts the D<sub>2</sub>O moderated thermal neutron spectrum (intensity maximum at approximately 1 Å) toward longer wavelengths. A liquid-nitrogen-cooled 15 cm long Be filter is installed in the beam path to remove fast neutrons (cutoff at 4 Å), and an additional 15 cm Bi filter removes the gamma radiation. The wavelength was set with the aid of a velocity selector (Dornier), using a high FWHM for the transmitted

beam with a wavelength resolution ( $\Delta\lambda/\lambda$ ) of 20% and maximized flux on the sample. The beam divergence was set by an input collimator (18.4 or 12.2 mm diameter) located 2.2 m from the sample, together with a sample collimator that was fixed to 4.9 mm. A 1.8 m long evacuated flight tube separates the collimators.

The solutions were filled in 1 mm quartz cuvettes, which were equipped with a detachable sidewall to facilitate a proper filling of samples of high viscosity. To avoid leakage of liquid from the cuvette, a gasket of viton was placed between the sidewalls and this resulted in a path length of the cell of 1.5 mm. The measuring cells were placed onto a copper-base for good thermal contact and mounted in the sample chamber. The chamber was evacuated to reduce air scattering. The detector was a  $128 \times 128$  pixel, 59 cm active diameter,  $^3\text{He}$ -filled RISØ type detector, which is mounted on rails inside an evacuated detector chamber. The distance was varied from 1.0 to 3.4 m, covering wavelengths between 5.1 and 10.2 Å. In all of the SANS measurements, deuterium oxide was used as a solvent instead of  $\text{H}_2\text{O}$  to obtain good contrast and low background for the neutron-scattering experiments.

Each complete scattering curve is composed of three independent series of measurement, using three different wavelength-distance combinations (5.1 Å/1.0 m, 5.1 Å/3.4 m, and 10.2 Å/3.4 m). These combinations were utilized to yield scattering vectors  $q = (4\pi n/\lambda) \sin(\theta/2)$  (where  $\lambda$  is the wavelength of the incident beam,  $\theta$  is the scattering angle, and  $n$  is the refractive index of the medium) in the range of  $0.008\text{--}0.25 \text{ Å}^{-1}$ . Standard reductions of the scattering data, including transmission corrections, were conducted by incorporating data collected from the empty cell, the beam without the cell, and the blocked-beam background. When relevant, the data were transformed to an absolute scale (coherent differential cross section ( $d\Sigma/d\Omega$ )) by calculating the normalized scattered intensity from direct beam measurements.<sup>22</sup>

## Results and Discussion

**Effects of Polymer Concentration at a Fixed Cross-linker Level.** Time evolution of the absolute value of complex viscosity (at a constant angular frequency of 10 rad/s) during gelation for different polymer concentrations at a fixed cross-linking density (12 mol %) is depicted in Figure 2a. The absolute values of  $\eta^*$  are higher as the polymer concentration rises, and the growth of  $|\eta^*|$  during the initial stage of the gelation process is more marked as the concentration increases. We can see that at longer times of reaction,  $|\eta^*|$  levels off probably due to the consumption of cross-linker molecules.

In the method developed by Winter and Chambon,<sup>23</sup> the gel point can be determined by observation of a frequency-independent value of  $\tan \delta$  ( $= G''/G'$ ) obtained from a multifrequency plot of  $\tan \delta$  versus time (see Figure 3). The common feature observed for all gelling alginate solutions is that the loss tangent is frequency dependent and decreases during gel formation, indicating that the systems become more and more elastic. The time of gelation is identified at

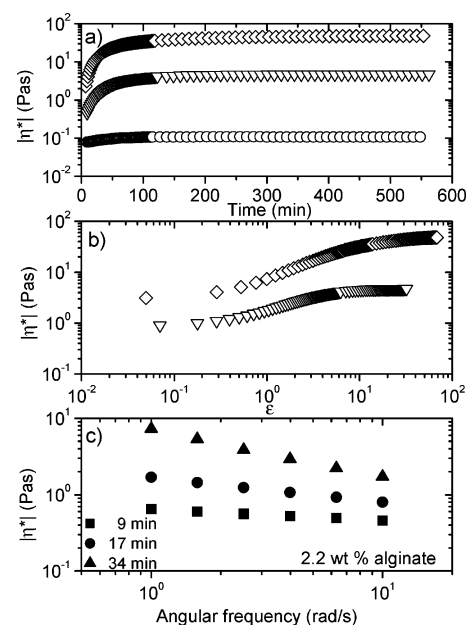


**Figure 2.** (a) Time evolution of the absolute value of complex viscosity (constant angular frequency of 10 rad/s) for the polymer concentrations of 1.5 wt % (○), 2.2 wt % (▽), and 3.0 wt % (◇) at a fixed cross-linker concentration of 12 mol %. (b) Plot of the absolute value of complex viscosity (log-log plot) as a function of the distance to the gel point ( $\epsilon$ ) for the polymer concentrations (2.2 and 3.0 wt %) forming gels in the presence of a fixed cross-linker concentration of 12 mol %. (c) Frequency dependence of the absolute value of complex viscosity (log-log plot) at different stages during the course of gelation for the polymer concentration indicated and at a cross-linker concentration of 12 mol %.

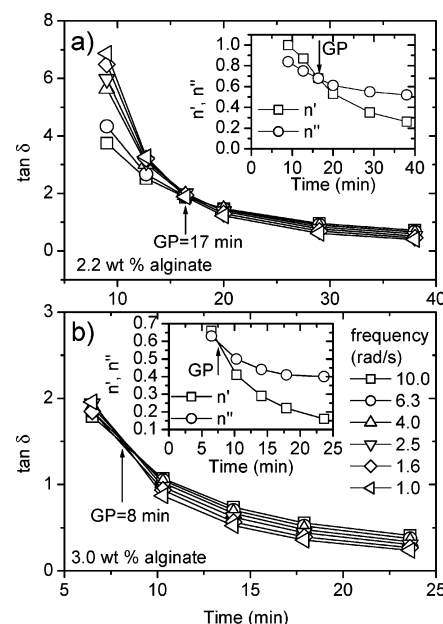


**Figure 3.** Viscoelastic loss tangent as a function of time for the polymer concentrations ((a) 2.2 wt % and (b) 3.0 wt %) and angular frequencies indicated at a cross-linker concentration of 12 mol %.

the point where a frequency-independent value of the loss tangent is first observed. An alternative method to determine the gelation point is to plot against time the “apparent” viscoelastic exponents  $n'$  and  $n''$  ( $G' \sim \omega^{n'}$ ;  $G'' \sim \omega^{n''}$ ) calculated from the frequency dependence of  $G'$  and  $G''$  at each time of measurement and observing a crossover where  $n' = n'' = n$  (see the inset plots of Figure 3). Both methods yield the same gelation times for the considered polymer



**Table 1.** Characteristic Parameters for Incipient Gels Obtained from Different Polymer Concentrations at a Cross-Linking Density of 12 mol %<sup>a</sup>

$C_{\text{alginate}}$ (wt %)	GP (min)	$n$			$S$ (Pa s <sup>n</sup> )
		$n'$	$n''$	$m$	
1.5	no gel				
2.2	17	$0.68 \pm 0.01$	$0.68 \pm 0.01$	-0.32	2.1
3.0	8	$0.51 \pm 0.02$	$0.54 \pm 0.01$	-0.47	12.9

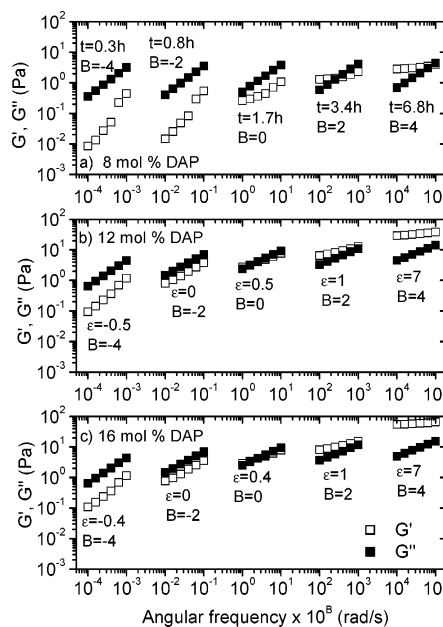
<sup>a</sup> The values of  $S$  have been calculated with the aid of eq 1.

concentrations. For the 1.5 wt % solution, no gelation is detected but only a viscosification of the solution, whereas at higher polymer concentrations, gels are formed and the time of gelation decreases with increasing polymer concentration (see Figure 3 and Table 1). At the low polymer concentration, the necessary connectivity of the sample-spanning network is probably not established. However, when the polymer concentration increases, a gel network is formed and the number of "active sites" for cross-linking of the polymer network rises, favoring a progressive faster gelation.

The time evolution of the absolute value of the complex viscosity beyond the gel point (where  $\epsilon = (t - t_g)/t_g$  is the relative distance from the gel point  $t_g$ ) is illustrated for the two gelling samples in Figure 2b. It is evident in the postgel region ( $\epsilon > 0$ ) that  $|\eta^*|$  is significantly higher and the viscosity enhancement is more pronounced for the highest polymer concentration. The reason for this difference in behavior at different polymer concentrations is probably that more entanglements<sup>24</sup> and effective intermolecular bridges, induced during the cross-linking reaction, are formed at higher polymer concentration. At a given cross-linker density, these results suggest that a higher polymer concentration promotes the formation of a stronger gel well beyond the gel point.

The frequency dependence of the absolute value of the complex viscosity, as measured in small amplitude oscillatory shear experiments, at different stages during the gelation process for a 2.2 wt % alginate solution at a cross-linker concentration of 12 mol % is displayed in Figure 2c. At early stages in the pregel domain, weak frequency dependence of  $|\eta^*|$  is found (liquidlike behavior), whereas as the gel evolves, a progressively stronger dependence is observed and a solidlike response is approached. This situation may be reminiscent of the model described previously<sup>24</sup> for near-critical gels. In this model, critical percolation applies to the reaction bath of unentangled chains in close proximity to the gel point, whereas beyond the gel point, trapped entanglements between network strands become important and raise the elastic response of the system.

The formation of incipient gels is usually explained theoretically in the framework of the percolation model, which describes the fraction of chemical bonds at the gel point to establish the connectivity of a sample-spanning cluster. In the interpretation of rheological features of incipient gels, e.g., the relaxation exponent  $n$ , two main theoretical models, which take into account the fractal geometry of polymer clusters and their intrinsic irregular structure, have been developed. Based on a suggested<sup>25,26</sup> isomorphism between the complex modulus and the electric

**Figure 4.** Frequency dependences of the storage modulus  $G'$  and the loss modulus  $G''$  at different stages of the gel-forming process for alginate solutions of 2.2 wt % with the cross-linker concentrations indicated. The curves have been shifted horizontally by a factor  $B$  of the value listed in the inset.

conductivity of a percolation network with randomly distributed resistors and capacitors, a value of  $n = 0.72$  was predicted. In the other approach,<sup>27</sup> the Rouse model, which assumes no hydrodynamic interaction between polydisperse polymeric clusters, together with percolation statistics yielded a value of  $n = 2/3$ . It is evident that the gel strength ( $S$ ) increases with polymer concentration at a fixed level of cross-linker addition (cf. Table 1). For the 2.2 wt % alginate concentration, the viscoelastic exponent  $n$  is in very good agreement with the Rouse model, whereas at higher polymer concentration, a lower value is observed. This trend is probably due to entanglement effects at higher polymer concentrations, and a similar behavior has been reported<sup>20,28,29</sup> for other chemically cross-linked polymer systems.

**Effect of Cross-Linker Density at a Constant Polymer Concentration.** In Figure 4, the frequency dependences of  $G'$  and  $G''$  at various stages during the gel evolution are shown for a 2.2 wt % alginate concentration at different levels of cross-linker addition. The curves have been shifted horizontally by a factor  $B$  (see the insets in Figure 4) to avoid overlap. All of the systems, except that with the lowest (8 mol %) cross-linker concentration, form gels. Up to the gel point,  $G'$  is always smaller than  $G''$ , and the frequency curves exhibit liquidlike behavior. After the gel point,  $G'$  rises and becomes larger than  $G''$ , which is a characteristic feature of the elastic response that becomes dominant in the postgel region. At the gel point, a power law frequency dependence of the dynamic storage modulus and loss modulus is observed with equal value of the power law exponent.

Figure 5a shows the time evolution of the absolute value of complex viscosity at different levels of cross-linker addition for alginate solutions of a constant polymer concentration (2.2 wt %) in the semidilute regime. The growth of  $|\eta^*|$  is faster and more pronounced as the cross-linker concentration increases and plateaulike regions appear at long

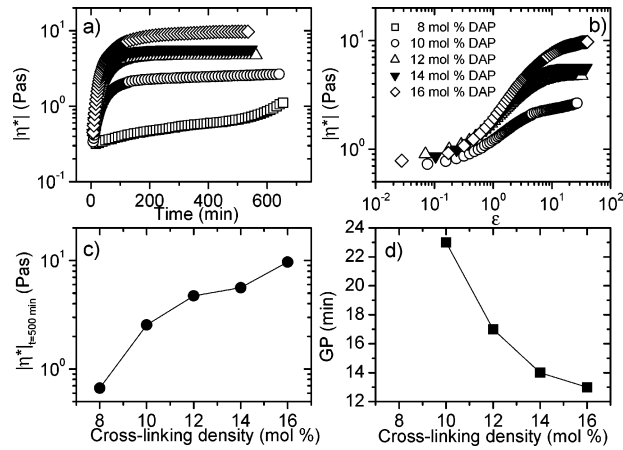


**Figure 5.** (a) Time evolution of the absolute value of complex viscosity (at a fixed angular frequency of 10 rad/s) during the gelation process of a 2.2 wt % alginate solution at the cross-linker concentrations indicated (no gel is formed at 8 mol % cross-linker). (b) Plot of the absolute value of complex viscosity (log–log plot) as a function of the distance to the gel point ( $\epsilon$ ) for a 2.2 wt % alginate solution at the cross-linker concentrations indicated. (c) The value of  $|\eta^*|$  at 500 min (in the postgel region for the gelling systems) as a function of cross-linker concentration. (d) The effect of cross-linker concentration on the gel point for a 2.2 wt % alginate solution. See text for details.

times (postgel regimes). The cease of the growth of  $|\eta^*|$  at long times suggests that the cross-linker agent is consumed and the gel network reaches a sort of steady state condition. At the lowest level of cross-linker addition (8 mol %), there is only a weak viscosification of the solution in the course of time and no gel is formed. At higher cross linker concentration, a further illustration of the enhancement of  $|\eta^*|$  as the distance from the gel point increases is displayed in Figure 5b, where  $|\eta^*|$  is plotted versus  $\epsilon$  for the gelling systems. These results indicate that the gel network is strengthened during a long time after the gel point, and the impact of this process is stronger as the cross-linker concentration increases.

The effect of cross-linker concentration on the absolute value of complex viscosity at a long time (500 min) is depicted in Figure 5c. The steady rise of  $|\eta^*|$  as the cross-linker concentration increases shows that “harder” gels are obtained at higher cross-linker density. The time of gelation decreases with increasing amount of cross-linking agent (see Figure 5d), because the probability of forming linkages with the cross-linker in the system increases.

The effect of cross-linker addition to alginate solutions of 2.2 wt % on the frequency dependence of  $|\eta^*|$  at different stages during the gel process is illustrated in Figure 6. It is interesting to note that the data points for the different cross-linker concentrations collapse onto each other, both in the pregel regime and for the incipient gels. This suggests that up to the gel point the viscoelastic response is practically the same for this polymer concentration, independent of the level of added cross-linker agent. However, in the postgel domain, a different situation appears, where a gradually more solidlike response emerges as the cross-linker concentration increases. This may indicate that the formation of additional cross-links and trapped entanglements in the gel network is promoted when the cross-linker concentration increases. The values of the power law exponent  $m$  reveal that the properties

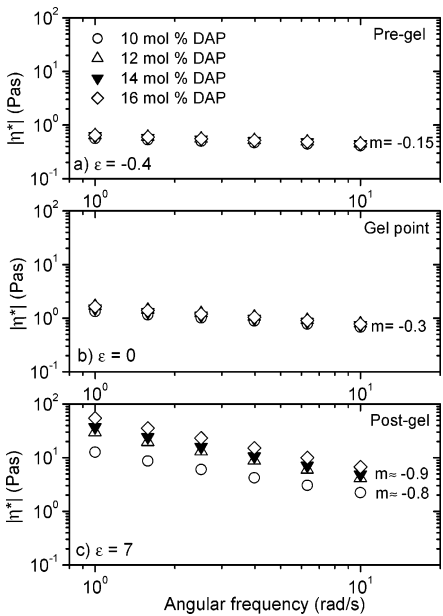


**Figure 6.** Frequency dependences of the absolute value of complex viscosity for alginate solutions of 2.2 wt % with different levels of cross-linker addition. The values of the power law exponent  $m$ , expressing the frequency dependence of  $|\eta^*|$ , are indicated.

**Table 2.** Characteristic Parameters for the Incipient Gels Obtained from 2.2 wt % Alginate Solutions with Different Amount of Cross-Linker Agent<sup>a</sup>

DAP (mol %)	GP (min)	$n$		$m$	$S$ (Pa s <sup><math>n</math></sup> )
		$n'$	$n''$		
8	no gel				
10	23	$0.71 \pm 0.01$	$0.71 \pm 0.01$	$-0.29$	1.6
12	17	$0.68 \pm 0.01$	$0.68 \pm 0.01$	$-0.32$	2.1
14	14	$0.71 \pm 0.02$	$0.69 \pm 0.02$	$-0.31$	1.9
16	13	$0.68 \pm 0.02$	$0.68 \pm 0.02$	$-0.32$	2.0

<sup>a</sup> The values of  $S$  have been calculated by means of eq 1.

of the samples change during the course of the gelation from almost liquidlike to virtually solidlike behavior ( $m \approx -1$ ) in the postgel zone (see inserts of Figure 6). This finding may indicate that the gel-forming process, via the Ugi reaction, proceeds over an extended period to produce a rigid gel and a high level of cross-linker addition promotes an augmented rigidity.

Some characteristic data of incipient gels from 2.2 wt % alginate solutions with different cross-linking density are presented in Table 2. We may note that the power law exponents ( $n$  or  $m$ ) are not affected by the level of cross-linker addition, but they assume constant values ( $n = 0.7$  or  $m = -0.3$ ), implying a unitary behavior of the gelling system at the gel point. The results presented in Table 2 show that the value of the viscoelastic exponent is consistent with that predicted from the percolation theory at all cross-linker concentrations, and the gel strength parameter is virtually independent of the level of cross-linker addition at this polymer concentration. The constancy of  $S$  and  $n$  with the level of cross-linker addition for this polymer sample may suggest that several entanglement couplings are formed at this polymer concentration, and an excess of cross-linker agent will only have a little influence on the architecture and strength of the incipient gel network. In a previous

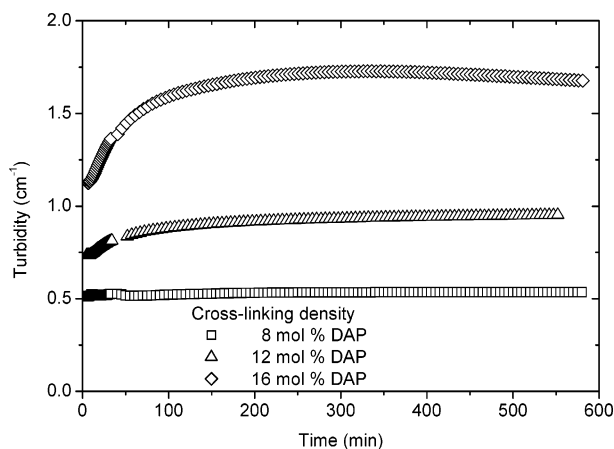


**Figure 7.** Time evolution of the turbidity (recorded at a wavelength of 500 nm) in the course of gelation for alginate solutions of 2.2 wt % with different levels of cross-linker addition.

study<sup>29</sup> of chemically cross-linked poly(vinyl alcohol) a similar trend was reported.

In Figure 7, the time evolution of the turbidity (at a wavelength of 500 nm) during gelation is depicted for alginate solutions of 2.2 wt % with different levels of cross-linker addition. For the nongelling sample with the lowest cross-linker density (8 mol %), the turbidity is practically constant over the considered time interval, whereas for the gelling systems, the general trend is that the turbidity and the growth of turbidity become more pronounced as the concentration of the cross-linker agent increases. At longer times (far in the postgel region), the curves level out. These findings suggest that gelation for this system is accompanied by the formation of large junction zones and this process continues far into the postgel region. The chemical cross-linking reaction probably leads to the formation of multichain associations, which give rise to enhanced turbidity. It is evident from these results that gelation of these systems is followed by enhanced turbidity and this probably reflects that the chemical cross-linking process induces large-scale heterogeneities of the sample. This is associated with the nonergodicity feature observed from dynamic light scattering experiments<sup>30</sup> in gels containing immobile inhomogeneities. In this context, it is interesting to note that theoretical studies<sup>31–33</sup> have established the interference between gelation and macroscopic phase separation. The enhanced turbidity during gelation may lend support to this prediction.

To gain insight into structural changes induced by the gelation process, we have carried out SANS experiments at different times on nongelling alginate solutions and gels (2.2 wt %) with various levels of cross-linker addition. Since the time of data accumulation in these SANS experiments is long and the times of gelation for these systems are quite short, it was not possible to monitor the intensity during the gel evolution but only at different times in the postgel domain.

Before the SANS results are discussed in detail, it may be instructive to give some basic aspects on differences in the intensity spectra between semidilute solutions and comparable gels. The excess scattering at low  $q$  values for polymer gels as compared to the equivalent semidilute solutions has been reported<sup>34–37</sup> from scattering experiments on polymer systems of various natures. To interpret the

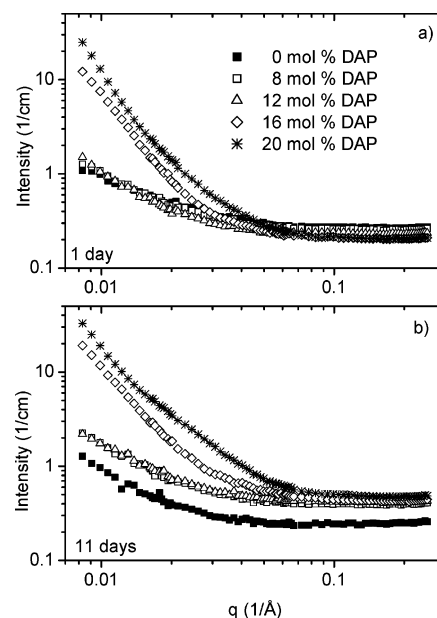


**Figure 8.** SANS scattered intensity  $I(q)$ , plotted versus the scattering vector  $q$  at different times for nongelling alginate solutions and gels (2.2 wt %) with various levels of cross-linker addition.

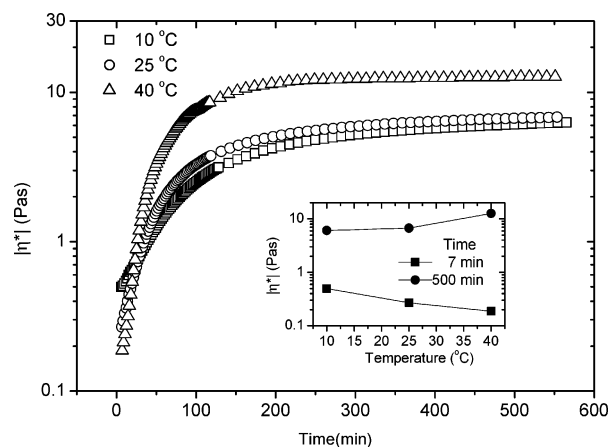
results, the total scattering intensity is frequently separated into contributions arising from thermal (dynamic) and quenched (static) fluctuations of polymer concentration. The thermal part portrays the fluctuations observed in a semidilute solution, whereas the quenched part is responsible for the excess of intensity scattered at low  $q$  from a corresponding gel. Both types of fluctuations contribute to the intensity measured in a SANS experiment on most gels. The thermal contribution reflects the liquidlike behavior of the gel and includes the dynamic spatial fluctuations of concentration that are continuously reformed through the Brownian motion of the scatters. The quenched part represents a spectrum of spatial fluctuations that are frozen-in by the quenched topological constraints. In the pioneering theoretical study by Stein,<sup>38</sup> it was argued that the scattering by a gel should reflect the nonuniformity of the cross-linking and that the excess scattering with respect to a corresponding solution should permit the characterization of the network inhomogeneity. Recent investigations<sup>35</sup> have indicated that the static fluctuations come from an inhomogeneous distribution of cross-links of the polymer network introduced during the gelation process, whereas the dynamic response comes from thermal fluctuations of the polymers between the cross-links. It is expected that the quenched fluctuations of polymer concentration are formed and gradually amplified under the introduction of cross-links in the system. The presence of cross-linking heterogeneities produces nearly frozen-in large-scale fluctuations of polymer concentration. The conjecture is that the cross-linking process intrinsically produces structural heterogeneities, which may be characterized<sup>35</sup> as a sort of “superstructure” consisting of “islands” or clusters of “frozen blobs” (regions of higher cross-linking density than the average of the system). Because of these structural nonuniformities, the structure of the gel network is inhomogeneous with distortions spanning over rather large scales.

Figure 8 shows SANS intensity profiles (plotted on a log–log scale) at different times (after 1 day and 11 days) for an

alginate sample (2.2 wt %) with different cross-linker concentrations (the gels are all in the postgel region). The measurements have been performed in a domain of  $q$  ranging approximately between 0.008 and 0.25 Å<sup>-1</sup>. The most conspicuous feature is the strong upturn of the scattering curves at low  $q$  values for the samples with high levels of added cross-linker agent. After 1 day (see Figure 8a), the scattering curves for the systems with cross-linker concentrations up to approximately 12 mol % collapse, within experimental accuracy, on the same curve. This finding suggests that there is no significant difference in the scattering profile between a semidilute solution and a gel (12 mol %) of the same polymer concentration as long as the cross-linker density is sufficiently low. This probably announces that the quenched heterogeneities in the polymer concentration profile are low. On the other hand, the upturn in intensity at lower  $q$  for the more cross-linked gels probably reflects an amplification of the spatial fluctuations of cross-linking density. This behavior is consistent with the strong turbidities observed at high cross-linker concentrations. At higher  $q$  values, the intensity curves are approximately superimposed (cf. Figure 8a) and do not reveal any significant difference in the local organization of the network structure. In view of the rheological results for the incipient gels, we may propose a fractal, percolation-like structure for the heterogeneous gel network. After the samples with added cross-linker have been standing in their sealed cells for several days (compare parts a and b of Figure 8), some noteworthy changes of the scattered intensity have taken place. A close inspection of the scattered intensity profiles at low  $q$  reveals that the upturns of the curves at all cross-linker concentrations are more pronounced than after 1 day. Furthermore, in contrast to the behavior after 1 day there is a significant difference between the curve representing the solution without cross-linker and the curves for the samples with low levels of added cross-linker (8 mol % and 12 mol %). These results suggest that the chemical cross-linking reaction continues over an extended period of time for the systems with added cross-linker agent, and the fraction of cross-linking molecules that are transformed into real inter-chain bridges increases in time and with rising cross-linking density. At high  $q$  values, the scattered intensity for the solution without added cross-linker is not affected by time, while the curves for the samples with different amount of cross-linker are shifted toward higher intensities at longer times. This finding indicates a time-induced change on a local scale of the system.

#### Effect of Temperature on the Rheological Properties.

Since the rate of the Ugi condensation reaction should be affected by temperature, we have also conducted rheological experiments at different temperatures during the gel-formation process of a 2.2 wt % alginate solution in the presence of 12 mol % of the cross-linker agent. The time evolution of the absolute value of complex viscosity during gelation at different temperatures is depicted in Figure 9. It is obvious from the insert that  $|\eta^*|$  in the pregel stage falls off with increasing temperature, whereas in the postgel domain,  $|\eta^*|$  rises as the temperature increases. During the gel formation process, the mobility of the polymer chains is expected to



**Figure 9.** Time evolution of the absolute value of complex viscosity (constant angular frequency of 10 rad/s) in the course of gelation at different temperatures for alginate solutions of 2.2 wt % with a cross-linker concentration of 12 mol %. The inset plot shows the temperature dependences of the absolute value of complex viscosity in the pre-gel domain (7 min) and in the postgel region (500 min).

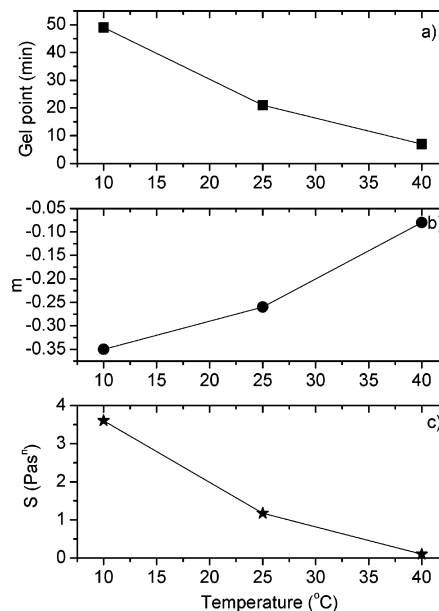


**Figure 10.** Effects of temperature on the gel point, exponent  $m$  (eq 5), and the gel strength parameter  $S$  (eq 1) for incipient gels of a 2.2 wt % alginate solution in the presence of 12 mol % of the cross-linker agent.

be promoted at elevated temperatures because the chain mobility is tied to solvent viscosity, which drops with increasing temperature. This effect may soften the elastic response of the system. In the postgel region, on the other hand, a temperature increase will speed up the cross-linking process and more cross-links are formed, making a “harder” gel. We should also bear in mind that the entropic elasticity of a postgel network rises as the temperature increases.

In Figure 10, some characteristic parameters for the incipient gels at different temperatures are summarized. The time of gelation decreases with increasing temperature, and this effect can probably be ascribed to the enhanced rate of the cross-linking reaction at higher temperatures, thereby establishing the necessary connectivity of the gel network earlier. The tendency of the power law exponent  $m$ , indicates that “softer” incipient gels (weaker elastic response) are formed at elevated temperatures. The decrease of the gel



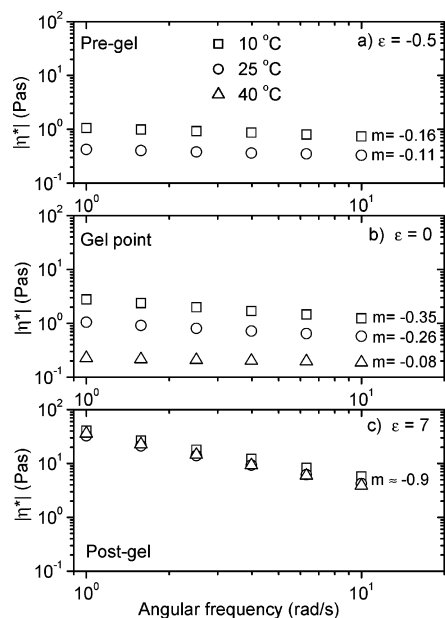


**Figure 11.** Frequency dependences of the absolute value of complex viscosity at different temperatures and stages during the gelation process for an alginate solution of 2.2 wt % with a cross-linker concentration of 12 mol %. The values of the power law exponent  $m$ , expressing the frequency dependence of  $|\eta^*|$ , are indicated.

strength parameter  $S$  with rising temperature may be due to the reduction of the network density and enhanced flexibility of the chains at the gel point.

Figure 11 shows the frequency dependences of  $|\eta^*|$  at different temperatures and stages during the gelation process for a 2.2 wt % alginate solution with a cross-linker concentration of 12 mol %. The small values of  $m$  in the pregel region reveal a liquidlike behavior with the most pronounced elastic response at the lowest temperature. Due to the very fast gel-forming process at the highest temperature, we were not able to obtain good and reproducible data at an early stage. At the gel point, the elastic response is strongest at the lowest temperature, where probably a more homogeneous gel network is formed. In the postgel domain, the data points almost collapse onto each other and the value of  $m \approx -0.9$ , suggesting a solidlike response. At this stage, the cross-linking reaction is probably to a large extent completed at all of the temperatures and the fraction of cross-linking molecules that are transformed into real interchain bridges is sufficiently high at all temperatures to produce a “hard” gel.

### Conclusions

In this work, we have investigated turbidity, structural, and rheological features of gelling alginate systems, prepared via the Ugi multicomponent condensation reaction. The effects of reaction temperature and polymer and cross-linker concentrations have been studied. The main results can be summarized in the following way: (1) The time of gelation decreases with increasing concentrations of polymer and cross-linker agent and higher temperatures speed up the gelation process. (2) At the gel point, the storage and loss moduli show a power law behavior,  $G' \propto G'' \propto \omega^n$ , with angular frequency  $\omega$ . At a fixed polymer concentration of

2.2 wt % in the semidilute regime, the value of  $n$  is consistent with that (0.7) predicted from the percolation theory at all of the considered levels of added cross-linker. Higher values of  $n$  are observed at elevated temperatures, and a higher polymer concentration yields a lower value than 0.7. (3) In the postgel domain, the strength of the gel increases progressively over a long time and gradually a solidlike response is approached. Elevated temperature and increasing polymer and cross-linker concentrations all favor the enhancement of the absolute value of complex viscosity beyond the gel point. (4) The time-dependent growth of viscoelasticity during the course of gelation of alginate is accompanied by an augmented turbidity. This effect is enhanced as the cross-linker concentration increases. The strong upturns of the scattered intensity at low  $q$  in the SANS intensity profiles reveal large-scale heterogeneities in the gels, and this effect develops in the course of time and is more accentuated at higher levels of cross-linker addition. (5) This study has demonstrated that the properties of the Ugi hydrogels, such as structure, transparency, gel point, and viscoelasticity can be tuned by changing the temperature and polymer and cross-linker concentrations.

**Acknowledgment.** H.B. and B.N. gratefully acknowledge support from the Norwegian Research Council (Project No. 148984/432). K.D.K. thanks the Marie Curie Industry Host Project (Contract No. G5TR-CT-2002-00089) for support, and B.N. and K.D.K. thank NANOMAT (Project No. 158550/431) for support.

### References and Notes

- (1) Ratner, B. D.; Hoffman, A. S. In *Hydrogels for Medical and Related Applications*; Andrade, J. D., Ed.; American Chemical Society: Washington, DC, 1976; Vol. 31, p 1.
- (2) DeRossi, D.; Kajiwar, K.; Osada, Y.; Yamauchi, A., Eds. *Polymer Gels Fundamentals and Biomedical Applications*; Plenum Press: New York, 1991.
- (3) Haug, A.; Larsen, B.; Smidsrød, O. *Acta Chem. Scand.* **1966**, *21*, 691.
- (4) Haug, A.; Myklestad, S.; Larsen, B.; Smidsrød, O. *Acta Chem. Scand.* **1967**, *21*, 768.
- (5) King, A. Brown Seaweed Extracts (Alginates). In *Food Hydrocolloids*; Glicksman, M., Ed.; CRC Press: Boca Raton, FL, 1982; Vol. II, p 115.
- (6) Draget, K. I.; Skjåk-Bræk, G.; Smidsrød, O. *Carbohydr. Polym.* **1994**, *25*, 31.
- (7) Atkins, E. D. T. *J. Polym. Sci. Part B, Polym. Lett.* **1971**, *9*, 311.
- (8) Xu, J. B.; Bartly, J. P.; Johnson, R. A. *J. Appl. Polym. Sci.* **2003**, *90*, 747.
- (9) Knott, J.; Rossbach, V. *Angew. Makromol. Chem.* **1980**, *86*, 203.
- (10) Wang, C.; Pailthorpe, M. T. *Text. Res. J.* **1989**, *59*, 671.
- (11) Eiselt, P.; Lee, K. Y.; Mooney, D. J. *Macromolecules* **1999**, *32*, 5561.
- (12) Lee, K. Y.; Rowley, J. A.; Eiselt, P.; Moy, E. M.; Bouhadir, K. H.; Mooney, D. J. *Macromolecules* **2000**, *33*, 4291.
- (13) Kong, H. J.; Wong, E.; Mooney, D. J. *Macromolecules* **2003**, *36*, 4582.
- (14) Ugi, I.; Lohberger, S.; Karl, R. The Passerini and Ugi Reactions. In *Comprehensive Organic Synthesis*; Trost, B. M.; Heathcock, C. H., Eds.; Pergamon: Oxford, U.K., 1991; Vol. 2, pp 1083–1107.
- (15) König, S.; Ugi, I. *Z. Naturforsch.* **1991**, *46b*, 1261.
- (16) Crescenzi, V.; Francescangeli, A.; Capitani, D.; Mannina, L.; Renier, D.; Bellini, D. *Carbohydr. Polym.* **2003**, *53*, 311.
- (17) de Nooy, A. E. J.; Masci, G.; Crescenzi, V. *Macromolecules* **1999**, *32*, 1318.
- (18) de Nooy, A. E. J.; Capitani, D.; Masci, G.; Crescenzi, V. *Biomacromolecules* **2000**, *1*, 259.
- (19) Smidsrød, O.; Draget, K. I. *Carbohydr. Eur.* **1996**, *14*, 6.
- (20) Scanlan, J. C.; Winter, H. H. *Macromolecules* **1991**, *24*, 47.

- (21) Winter, H. H. *Prog. Colloid Polym. Sci.* **1987**, 75, 104.
- (22) Wignall, G. D.; Bates, F. S. *J. Appl. Crystallogr.* **1987**, 20, 28.
- (23) Winter, H. H.; Chambon, F. *J. Rheol.* **1986**, 30, 367.
- (24) Rubinstein, M.; Colby, R. H. *Macromolecules* **1994**, 25, 3184.
- (25) De Gennes, P. G. *Scaling Concepts in Polymer Physics*; Cornell University Press: Ithaca, NY, 1979.
- (26) Alexander, S. *J. Phys. (Paris)* **1984**, 45, 1939.
- (27) Martin, J. E.; Adolf, D.; Wilcoxon, J. P. *Phys. Rev. Lett.* **1988**, 61, 2620; *Phys. Rev. A* **1989**, 39, 1325.
- (28) Koike, A.; Nemoto, N.; Takahashi, M.; Osaki, K. *Polymer* **1994**, 35, 3005.
- (29) Kjøniksen, A.-L.; Nyström, B. *Macromolecules* **1996**, 29, 5215.
- (30) Joosten, J. G. H.; Geladé, E. T. F. *Phys. Rev. A* **1990**, 42, 2161.
- (31) Tanaka, F.; Stockmayer, W. H. *Macromolecules* **1994**, 27, 3943.
- (32) Ishida, M.; Tanaka, F. *Macromolecules* **1997**, 30, 3900.
- (33) Semenov, A. N.; Rubinstein, M. *Macromolecules* **1998**, 31, 1373.
- (34) Lal, J.; Basile, J.; Bansil, R.; Boué, F. *Macromolecules* **1993**, 26, 6092.
- (35) Bastide, J.; Candau, S. J. In *Physical Properties of Polymeric Gels*; Cohen Addad, J. P., Ed.; John Wiley & Sons, Ltd: Chichester, U.K., 1996; pp 143–295.
- (36) Rouf-George, C.; Munch, J.-P.; Schosseler, F.; Pouchelon, A.; Beinert, G.; Boué, F.; Bastide, J. *Macromolecules* **1997**, 30, 8344.
- (37) Hecht, A.-M.; Horkay, F.; Geissler, E. *J. Phys. Chem. B* **2001**, 105, 5637.
- (38) Stein, R. S. *J. Polym. Sci. B* **1969**, 7, 657.

BM049947+